

# Effect of Flow Holes on Heat Release Performance of Extruded-type Heat Sink

Jung Hyun Kim, Gyo Woo Lee

**Abstract**—In this study, the enhancement of the heat release performance of an extruded-type heat sink to prepare the large-capacity solar inverter thru the flow holes in the base plate near the heat sources was investigated. Optimal location and number of the holes in the baseplate were determined by using a commercial computation program. The heat release performance of the shape-modified heat sink was measured experimentally and compared with that of the simulation. The heat sink with 12 flow holes in the 18-mm-thick base plate has a 8.1% wider heat transfer area, a 2.5% more mass flow of air, and a 2.7% higher heat release rate than those of the original heat sink. Also, the surface temperature of the base plate was lowered 1.5°C by the holes.

**Keywords**—Heat Sink, Forced Convection, Heat Transfer, Performance Evaluation, Flow Holes.

## I. INTRODUCTION

A SOLAR inverter is a power-electronic circuit that converts dc voltage from a solar array panel to ac voltage that can be used to power ac loads such as home appliances, lighting and power tools [1]. The inverter has insulated-gate bipolar transistors (IGBTs) which are high converting speed power semiconductors and are essential element in the inverter. The power loss from the IGBT turns into heat and increases the junction temperature inside the chip. This heat degrades the characteristics of the device and shortens its life. So, it is important to allow the heat produced from the chip junction to escape outside to lower the junction temperature [2], [3]. IGBTs are packed with the heat release system like heat sink.

Lots of works related with various heat sinks were done. In 2004, Lee [4] reported the design process with using both experiment and simulation results. He showed that the differences between them were less than 10% for the 400 kW IGBT inverter. Similarly, Jeon et al. [5] examined the effects of temperature increment of the serially aligned heat sources on the heat release performance of the tunnel-type air-cooled heat sink. Also, they presented the example design of heat release system by using the empirical relation came from the experiment. While, Kim et al. [6] developed the heat release system for the deep-focused solar cell modules having heat spreaders and heat sinks. They also reported the empirical relation can be used for the estimation of heat release performance of the natural convection heat sink. In 1996,

Shaukatullah et al. [7] reported an optimized design of pin-fin heat sink for use in low velocity applications where there is plenty of open space around for the air to bypass the heat sink. While, in 2002, Kim et al. [8] investigated the thermal performance of several heat sinks such as extruded, aluminum foam, and layered one. Lee [9] reported the optimization of heat sink with pressure drop and heat transfer area. The pressure drops and heat transfer were varied by changing the number of fins. Riu et al. [10] evaluated the performance of a heat sink with strip-shaped fin, and tried to determine the optimal geometry.

The extrude-type heat sinks are used widely in the several fields of heat release systems. Compared with a swaged-type heatsink which might be assembled together with base plates and fins an extruded-type heat sink has much better heat transfer property. While in the cases of large-scaled heat release systems, swaged-type heat sinks are used instead of the extruded-type heat sinks due to their fabrication limit related with the extrusion pressure.

In this study, we want to enhance the heat release performance of an extruded-type heat sink to prepare the large-capacity solar inverter thru the flow holes in the base plate near the heat sources. Optimal location and number of the holes in the base plate are determined by using a commercial computation program. The heat release performance of the shape-modified heat sink is measured experimentally and compared with that of the simulation.

## II. EXPERIMENTAL METHOD AND SIMULATION

### A. Experimental Setup

Fig. 1 shows the experimental setup used in this study including three heat sources, two fans, four thermocouples, and in/out ducts. The first and the second figure are showing top and side views indicating the locations of those components. The last figure shows the sectional views of this experimental setup. The experimental setup is consist of a heat sink, three heat sources, two induction fans (6314/2TDHHP, Ebmpapst Inc.), inlet ( $\Phi 0.25\text{m}$ ) and exit ( $\Phi 0.20\text{m}$ ) flow ducts, data acquisition system for temperatures and air velocity, several thermocouples and others. Almost the same experimental setup as our previous work [11] was used.

Three aluminum blocks having six cartridge heaters on the upper plate of the heat sink used as substitutes for IGBTs in the commercial inverter. They have a total power consumption of 1905Watt, and have a dimension of 60mm (W) x 140mm (L) x 20mm (H) in each. Thermal grease (OT-201, Omega Co.) was used on the surface of cartridge heaters and spaces between

J. H. Kim, Graduate School Student is with the Division of Mechanical DesignEngineering, Chonbuk National University, Jeonju, Jeonbuk 561-756, South Korea (e-mail: chemist@jbnu.ac.kr).

G. W. Lee, Corresponding Author, Associate Professor is with the Division of Mechanical DesignEngineering, Chonbuk National University, Jeonju, Jeonbuk 561-756, South Korea (e-mail: gwlee@jbnu.ac.kr).

aluminum blocks and upper plate of heat sink to enhance the heat transfer among them. Those heating blocks are covered with heat insulating fabric. The central block was positioned 115mm apart from the front of heat sink. The space between the central block and the other two blocks are 60mm each.

The cooling air is flowed into the heat sink from the ambient, heated by the base plate and fins, and then exhausted to the outside thru the duct. Several dot marks near the heat sink in Fig. 1 are locations of thermocouples for measuring the heat transfer thru the heat sink. The T-type thermocouples are made of fine bare wire (TG-T-36-500, Omega Co.) and used after the calibration. The temperatures from the thermocouples were converted to digital data thru the A/D converting device (34970A with 34902A module, Agilent Technologies) and saved in the computer [11].

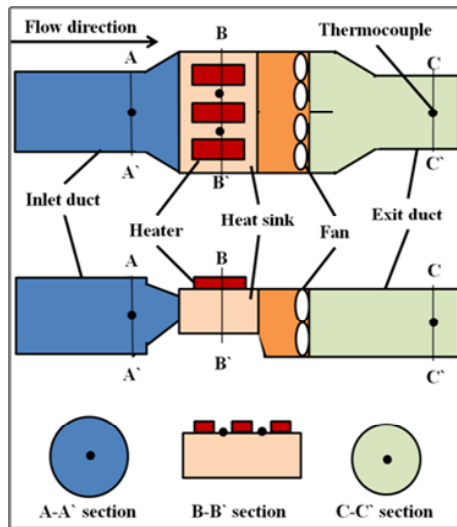


Fig. 1 Experimental setup [11]

Photos of the extruded-type heat sinks having 47 fins used in this study are shown in Fig. 2. Because it is manufactured by extrusion of aluminum (AL6061), fins and base plate are a single body. Acrylonitrile lower plate is fabricated separately and assembled together. Detailed specifications of the heat sink are written in Table I.

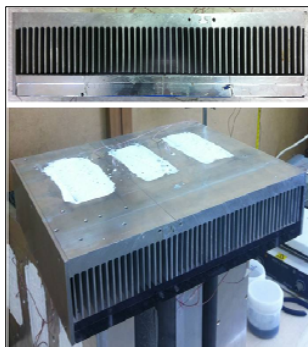


Fig. 2 Photos of the heat sink

TABLE I  
SPECIFICATION OF THE HEAT SINK

|                    |                      |
|--------------------|----------------------|
| Number of fins     | 47                   |
| Heat sink length   | 325 mm               |
| Heat sink width    | 400 mm               |
| Heat sink height   | 100 mm               |
| Thickness of base  | 18 mm                |
| Fin spacing        | 8.5 mm               |
| Thickness of fin   | 2.2 mm               |
| Height of fin      | 55 mm                |
| Heat transfer area | 1.810 m <sup>2</sup> |

### B. Experimental Method

In this experiment, the heat from the heat source was released thru the heat sink by the forced convection using two fans. The heat release performance of the heat sink was measured by using a heat input of the three heaters on the heat sink and an amount of heat transfer thru the heat sink. The measured heat input, that is, the electricity consumption of the three heaters on the heat sink, was 1904.8 Watt. The temperature difference between inlet and exit temperatures of cooling air gave the information about the amount of heat release thru the heat sink.

Temperature measurement was done every 5 seconds. After 90 minutes from the fan operation, the system was fully reached the first steady state. Since the steady state, averaged inlet and exit air temperatures and the differences were measured and calculated during another 90 minutes as shown in Fig. 3. The second steady state might be reached in 20 minutes from the heater operation in Fig. 3. In this experiment, when the standard deviation of 10-minute averaged temperature was less than 0.5°C we considered it as the steady state. The same experimental procedure was used as our previous work [11].

Using a simple heat transfer equation as below [12], the calculation for the amount of heat transfer thru the heat sink was done. Here,  $\dot{Q}$ ,  $\dot{m}_{air}$ ,  $C_p$ , and  $\Delta T$  denote heat transfer rate (W), mass flow rate of air (kg/s), specific heat at constant pressure (J/kg · K), and temperature difference between inlet and exit air thru the heat sink (K), respectively.

$$\dot{Q} = \dot{m}_{air} \cdot C_p \cdot \Delta T \quad (1)$$

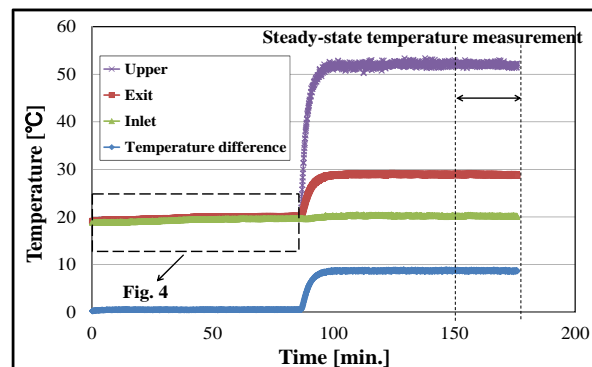


Fig. 3 Distributions of transient temperatures of a heat sink showing the period of steady-state temperature

TABLE II

| RATIOS OF MEAN AND MAXIMUM VELOCITIES WITH REYNOLDS NO |       |        |        |        |        |        |
|--|-------|--------|--------|--------|--------|--------|
| $Re_d$   | 4000  | $10^4$ | $10^5$ | $10^6$ | $10^7$ | $10^8$ |
| $V/u_{max}$  | 0.794 | 0.814  | 0.852  | 0.877  | 0.895  | 0.909  |

Two fans that were used in this experiment have a maximum flow rate (that is, zero pressure drop) of  $710 \text{ m}^3/\text{hr}$  in each. Fans were installed parallel as shown in Fig. 1. To calculate the mass flow rate, the air velocity induced by the fans thru the inlet duct was measured at the center of the location of 1m behind the entrance of inlet duct by the velocity meter (Model 8386, TSI Inc.). With an assumption of fully-developed flow, the mass flow rate might be calculated from density of air, cross sectional area of duct and averaged velocity of air. The averaged air velocity can be calculated from the measured maximum air velocity and the corresponding conversion ratio varied with Reynolds number as follows in Table II [13]. In this experiment, the conversion ratio ranged from 0.827 to 0.829. Generally, to use the fully-developed flow assumption the ratio of length to diameter (L/D) of duct should exceed 20. In this experiment, due to the restriction of indoor space and the big pressure drop might be caused by the long inlet duct, the ratio is maintained less than 6. So, the actual mass flow of the air thru the heat sink can be slightly larger than that of measured in this experiment [11].

### C. Numerical Simulation

A numerical simulation was done using a commercial flow simulation program (Fluent ver.6). At first, the 47-finned heat sink (shown in Fig. 2 and Table I) without having holes in the base plate was modeled and the results were compared with those of experiment. The aim of the simulation is to find out the optimal number and location of flow holes in the base of heat sink. Taking the base thickness into consideration the hole diameter was determined as 12mm. Three geometries of heat sink base with 8, 14, and 17 holes are shown in Fig. 4. The center of the first hole is positioned 40mm apart from the edge of base plate. The distance between centers of neighboring holes is 20mm. In the cases of heat sinks with 8 and 14 holes, the holes near the heat sources are neglected to ensure the conduction path from base plate to fins.

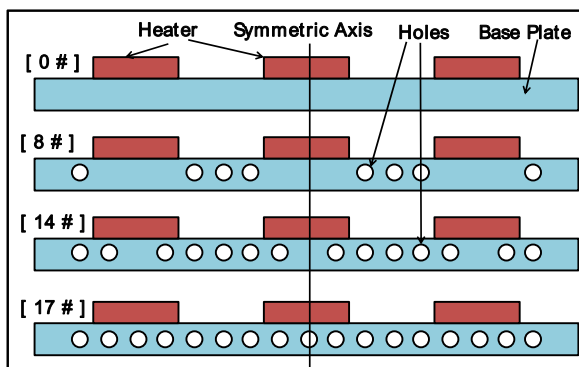


Fig. 4 Cross sectional views of base plates of heat sinks showing flow holes

TABLE III

| CROSS SECTIONAL AREAS AND MEASURED MASS FLOWS FOR HEAT SINKS WITH 38 AND 47 FINS |        |        |
|--|--------|--------|
| Number of fins   | 38     | 47     |
| Sectional area [ $\text{m}^2$ ]  | 0.0198 | 0.0163 |
| Mass flow [ $\text{kg/s}$ ]  | 0.2129 | 0.1993 |

TABLE IV

| CROSS SECTIONAL AREAS AND EXPECTED MASS FLOWS FOR HEAT SINKS WITH 8, 14, AND 17 HOLES |        |        |        |
|---|--------|--------|--------|
| Number of holes[#]  | 8      | 14     | 17     |
| Sectional area [ $\text{m}^2$ ]   | 0.0172 | 0.0179 | 0.0182 |
| Expected mass flow [ $\text{kg/s}$ ]  | 0.2029 | 0.2052 | 0.2070 |

The ambient temperature was remained constant throughout the simulations, but the flow rates of air thru the heat sink might be varied with changed pressure drop due to the altered cross sectional areas of the heat sinks having flow holes. The relation between cross sectional areas and mass flow rates of air for the cases of 38- and 47-finned heat sinks was used to estimate the air flow rates in the simulation as shown in Table III. On the basis of Table III, cross sectional areas and mass flow rates of air used as input data in this simulation were calculated and presented in Table IV.

## III. RESULTS AND DISCUSSION

### A. Numerical Simulation for Optimal Heat Release

The heat release rate, surface temperature of base plate between heat sources, air mass flow rate of the 47-finned heat sink shown in Fig. 2 and Table I were measured as 81.6%,  $51.4^\circ\text{C}$ , and  $11.9 \text{ kg/min}$ , respectively. The measured mass flow rate was used as an input for the simulation. Through the simulation the heat release rate and base plate temperature were 82.8% and  $51.2^\circ\text{C}$ , respectively. It was believed that these small differences between experiment and simulation results might verify that the boundary conditions for the simulation worked properly.

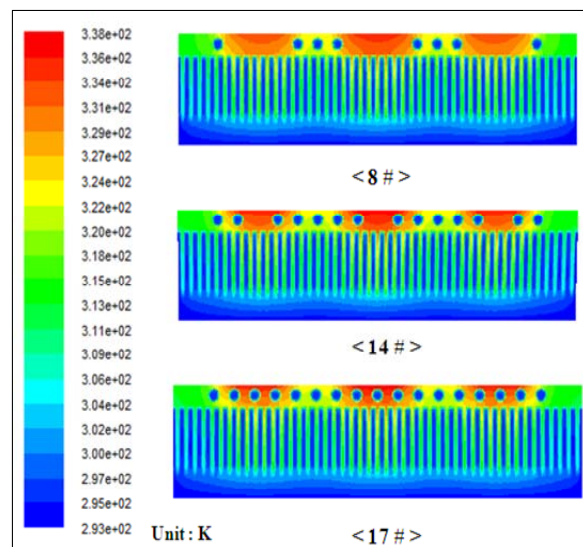


Fig. 5 Temperature contours of heat sinks with flow holes

TABLE V  
SUMMARY OF NUMERICAL SIMULATION OF HEAT SINKS WITH HOLES

| Number of holes                      | 0    | 8    | 14   | 17   |
|--------------------------------------|------|------|------|------|
| Ambient temperature [°C]             |      |      | 20.0 |      |
| Heat transfer area [m <sup>2</sup> ] | 1.81 | 1.91 | 1.98 | 2.02 |
| Temperature of base plate [°C]       | 51.2 | 49.8 | 49.3 | 49.4 |
| Mass flow rate [kg/min]              | 11.9 | 12.1 | 12.3 | 12.4 |
| Heat release [%]                     | 82.8 | 83.0 | 83.2 | 83.3 |

To find out the optimal locations of the holes in base plate the simulation was done regarding the locations of holes as shown in Fig. 4 and estimated air flow rates presented in Table IV. The steady-state temperature contours of the heat sinks were shown in Fig. 5. The results of several simulations were presented in Table V. As the number of holes increased the heat transfer areas and mass flow rates were increased. The heat release rates were also increased but not much. The temperatures of the base plate were slightly decreased with increase the number of holes but stagnated for the case of heat sink having 17 holes. Based on the results in Table V, it is believed that the flow holes in base plate were helpful to increase the mass flow and heat transfer area but detrimental to thermal conduction from base to fins. Taking both of the merit and demerit of the holes into consideration, we believe that the 14-holed heat sink might have the best heat release performance.

#### B. Heat Release Performance of the Modified Heat Sink

On the basis of simulation results the fabrication of 14-holed heat sink were tried, but it was impossible to make a hole in the connecting section of the extruded-type heat sink as shown in Fig. 2. So, the fifth hole in the second figure of Fig. 4 was neglected. To maintain the symmetry of the heat sink the tenth hole was also excluded. The prototype heat sink having 12 flow holes was fabricated and the front view showing holed base and fins was seen in Fig. 6.

Using the prototype heat sink the same experiment and simulation as those of the original heat sink were done. Results were summarized as below in Table VI. On the basis of the experimental data of the 0-holed original heat sink, the air mass flow, heat transfer area, and heat release rate of the 12-holed shape-modified heat sink were enhanced 2.5%, 8.1%, and 2.7%, respectively. The surface temperature of the base plate between heat sources was lowered 1.5°C by the holes.

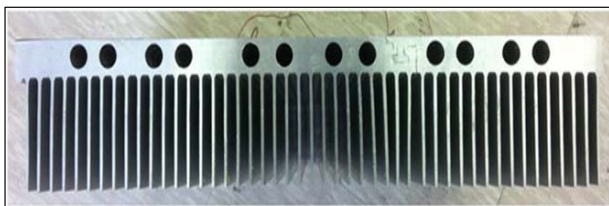


Fig. 6 Front view of the heat sink showing 12 flow holes in base

TABLE VI  
SUMMARY OF EXPERIMENTAL AND SIMULATION OF HEAT SINK WITH HOLES

| Heat Sink with 47 fins   | Without hole | With 12 holes (experiment) | With 12 holes (simulation) |
|--------------------------|--------------|----------------------------|----------------------------|
| Inlet temperature [°C]   | 20.4         | 20.6                       | 20.0                       |
| Temperature of base [°C] | 51.4         | 49.9                       | 49.4                       |
| Mass flow rate [kg/min]  | 11.9         | 12.2                       | 12.2                       |
| Heat release [%]         | 81.6         | 83.8                       | 83.1                       |

#### IV. CONCLUSION

In this study, the enhancement of the heat release performance of an extruded-type heat sink thru the flow holes in the base plate near the heat sources was investigated. Optimal location and number of the holes in the base plate were determined by using a commercial computation program. The heat release performance of the shape-modified heat sink is measured experimentally and compared with that of the simulation.

On the basis of the experimental data of the 0-holed original heat sink, the air mass flow, heat transfer area, and heat release rate of the 12-holed shape-modified heat sink were enhanced 2.5%, 8.1%, and 2.7%, respectively. The surface temperature of the base plate between heat sources was lowered 1.5°C by the holes. Based on the results, it is believed that the flow holes in the base plate of heat sink were helpful to increase the air mass flow and heat transfer area but detrimental to the thermal conduction from base plate to fins.

#### ACKNOWLEDGMENT

This research was financially supported by the Ministry of Trade, Industry & Energy (MOTIE), Korea Institute for Advancement of Technology (KIAT) and Honam Institute for Regional Program Evaluation through the Promoting Regional specialized Industry.

#### REFERENCES

- [1] W. Chou, "Choose Your IGBTs Correctly for Solar Inverter Applications," *Power Electronic Technology*, August, pp. 20-23, 2008.
- [2] E. Santi, A. Caiafa, X.Kang, J. L. Hudgins, and P. R. Palmer, D. Goodwine, and A. Monti, "Temperature Effects on Trench-Gate Punch-Through IGBTs," *IEEE Trans. on Industry Applications*, Vol. 40, No. 2, pp. 472-482, 2004.
- [3] K. S. Oh, IGBT Basics 1 Fairchild Semiconductor, Application Note 9016, Feb., p. 15, 2001.
- [4] J. W. Lee, "Design of a Heat Dissipation System for the 400kW IGBT Inverter," *The Trans. of the KIPE*, Vol. 9, No. 4, pp. 350-355, 2004.
- [5] C. S. Jeon, Y. K.Kim, J. Y. Lee, and S. H.Song, "Cooling of an In-line Array of Heat Sources with Air-Cooled Heat Sinks," *Trans. Korean Soc. Mech. Eng. B*, Vol. 22, No. 2, pp. 229-234, 1998.
- [6] T. H.Kim, K. H.Do, B. I.Choi, Y. S. Han, and M. B. Kim, "Development of a Cooling System for a Concentrating Photovoltaic Module," *Trans. Korean Soc. Mech. Eng. B*, Vol. 35, No. 6, pp. 551-560, 2011.
- [7] H. Shaukatullah, W. R.Storr, B. J. Hansen, and M. A. Gaynes, "Design and Optimization of Pin Fin Heat Sinks for Low Velocity Applications," *IEEE Trans. on Components, Packaging and Manufacturing Technology-Part A*, Vol. 19, No. 4, pp. 486-494, 1996.
- [8] J. H. Kim, J. H. Yun, and C. S. Lee, "An Experimental Study on the Thermal Resistance Characteristics for Various Types of Heat Sinks," *SAREK*, Vol. 14, No. 8, pp. 676-682, 2002.
- [9] S.Lee, "Optimum Design and Selection of Heat Sinks," *IEEE Trans. Components, Packaging and Manufacturing Technology-Part A*, Vol. 18, No. 4, pp. 812-817, 1995.
- [10] K. J. Riu, C. W. Park, H. W. Kim, and C. S.Jang, "Cooling Characteristics of a Strip Fin Heat Sink," *Trans. Korean Soc. Mech. Eng. B*, Vol. 29, No.

- 1, pp. 16~26, 2005.
- [11] J. H. Kim, and G. W. Lee, "Performance Evaluation of Extruded-Type Heat Sinks Used in Inverter for Solar Power Generation," *World Academy of Science, Engineering and Technology*, Vol. 84, pp. 857~860, 2013.
- [12] F. P. Incropera, D. P. DeWitt, T. L. Bergman, and A. S. Lavine, "Introduction to Heat Transfer," 5th ed., John Wiley and Sons, 2006.
- [13] F. M. White, "Fluid Mechanics," 5th ed., McGraw-Hill, 2011.